Stimulation of endogenous neurogenesis by anti-EFRH immunization in a transgenic mouse model of Alzheimer's disease

Maria Becker, Vered Lavie, and Beka Solomon*

Department of Molecular Microbiology and Biotechnology, George S. Wise Faculty of Life Sciences, Tel-Aviv University, Ramat Aviv, Tel-Aviv 69978, Israel

Communicated by Ephraim Katchalski-Katzir, Weizmann Institute of Science, Rehovot, Israel, November 29, 2006 (received for review June 15, 2006)

Neurogenesis is a subject of intense interest and extensive research, but it stands at the center of a bitter debate over ethical and practical problems. Neurodegenerative diseases, such as Alzheimer's disease (AD), accompanied by a shifting balance between neurogenesis and neurodegeneration, are suitable for stimulation of neurogenesis for the benefit of diseased patients. We have previously shown that Abs against the EFRH sequence of β-amyloid peptide (AβP) prevent aggregation and disaggregate AβP both *in vitro* and *in vivo*. EFRH, located in the soluble tail of the N-terminal region, acts as a regulatory site controlling both solubilization and disaggregation processes in the AβP molecule. Here we show that anti-EFRH immunotherapy of a platelet-derived amyloid precursor protein transgenic mouse model of AD stimulates endogenous neurogenesis, suggested by elevated numbers of BrdU-incorporated cells, most of which are colocalized with a marker of mature neurons, NeuN. These newly born neurons expressed the activity-dependent gene Zif268, indicating their functional integration and participation in response to synaptic input in the brain. These findings suggest that anti-amyloid immunotherapy may promote recovery from AD or other diseases related to AβP overproduction and neurotoxicity by restoring neuronal population, as well as cognitive functions in treated patients.

amyloid β | immunotherapy | neurodegenerative diseases | platelet-derived amyloid precursor protein transgenic mice

Adult brain neurogenesis continues throughout life, helping to maintain nervous-system integrity. It involves neural stem cells (NSC) found in the two principal neurogenic regions: the subgranular zone (SGZ) of the dentate gyrus (DG), which generates the hippocampal interneurons (1), and the forebrain subventricular zone (SVZ) of the lateral ventricles, which migrate to the olfactory bulb (2–5). NSC are self-renewing, multipotent cells that generate neurons, astrocytes, and oligodendrocytes in the nervous system. These progenitor cells migrate to their final locations and functions, becoming neurons or glia depending on their microenvironment (reviewed in ref. 6). Alterations in the microenvironment may affect neurogenesis, rendering it ectopic or even blocked, thus leading to deficits in learning and memory (7–9).

One of the major pathological features of the Alzheimer's disease (AD) patient's brain tissue is the abundance of amyloid plaques, composed of β-amyloid peptide (AβP) (10). The amyloid cascade hypothesis states that overproduction of AβP, or failure to clear it, leads to AD primarily through amyloid deposition associated with cell death, which is reflected in memory impairment (11, 12).

During the last decade, anti-AβP immunization proved effective in amyloid burden reduction and improvement of memory deficits in AD transgenic (Tg) mice (13, 14) and in AD patients (15). A few main mechanisms are considered to be involved in immunotherapy efficacy: catalytic dissolution of Aβ fibrils (16); opsonization of amyloid by the Ab and subsequent phagocytosis by microglia (17); and the peripheral sink hypothesis (18). A recent report (19) supports all of these mechanisms and suggests that they may act synergistically.

By using phage-peptide libraries displaying random combinatorial peptides the EFRH epitope, located at position 3–6 of the N terminus of AβP, was identified as the minimal key sequence that controls peptide aggregation (20, 21). EFRH site-directed Abs were generated and proved in *in vitro* studies to prevent and suppress aggregation of AβP, as well as to resolubilize already preformed toxic amyloid fibrils (16, 22). In *in vivo* studies, immunization of various AD-Tg mice, using the EFRH as antigen, was effective in reducing the number of AβP plaques and the pathology associated with AD (23, 24). EFRH epitope is available for Ab binding whether AβP is in a soluble or aggregated state, and locking of this epitope by mAbs affects the dynamics of the whole molecule.

Here we show EFRH site-directed immunization of platelet-derived amyloid precursor protein (PDAPP) Tg mice, a model of AD, which alleviated AβP pathology and stimulated brain-intrinsic neurogenesis, as manifested by the elevated number of cells incorporating BrdU ($BrdU^+$). Most of these cells also express the mature neuronal marker NeuN and the activity-dependent gene Zif268 (25), thus appearing to be functional and, probably, integrated into the brain circuits.

PDAPP Tg mice demonstrated pathology similar to that of the early-onset and aggressive form of autosomal dominant AD (26). Age-dependent increase in amyloid pathology in PDAPP mice inflicts stress/injury, leading to ectopic neurogenesis, as recently shown in DG of 1-year-old mice (27). The recruitment of endogenous NSC in response to injury failed to lead to substantial recovery; however, we show here that the immunotherapeutic strategy stimulates functional neurogenesis.

Modulation of endogenous adult neurogenesis by immunotherapy for AD treatment may lead to development of new strategies for neurodegenerative disease treatment.

Results

The anti-EFRH immunization effect on alleviation of AD-associated brain pathology, i.e., reduction of amyloid burden and brain inflammation, is presented in supporting information (SI) Fig. 5.

BrdU Incorporation and Neurogenesis. BrdU incorporation was examined in PDAPP Tg treated and untreated mice 41 days after

Author contributions: M.B. and V.L. contributed equally to this work; V.L. and B.S. designed research; M.B. and V.L. performed research; M.B., V.L., and B.S. analyzed data; and M.B., V.L., and B.S. wrote the paper.

The authors declare no conflict of interest.

Abbreviations: AD, Alzheimer's disease; AβP, β-amyloid peptide; Tg, transgenic; PDAPP, platelet-derived amyloid precursor protein; SGZ, subgranular zone; DG, dentate gyrus; SVZ, subventricular zone; NSC, neural stem cell; GFAP, glial fibrillary acidic protein.

*To whom correspondence should be addressed. E-mail: beka@post.tau.ac.il.

This article contains supporting information online at www.pnas.org/cgi/content/full/0610180104/DC1.

© 2007 by The National Academy of Sciences of the USA

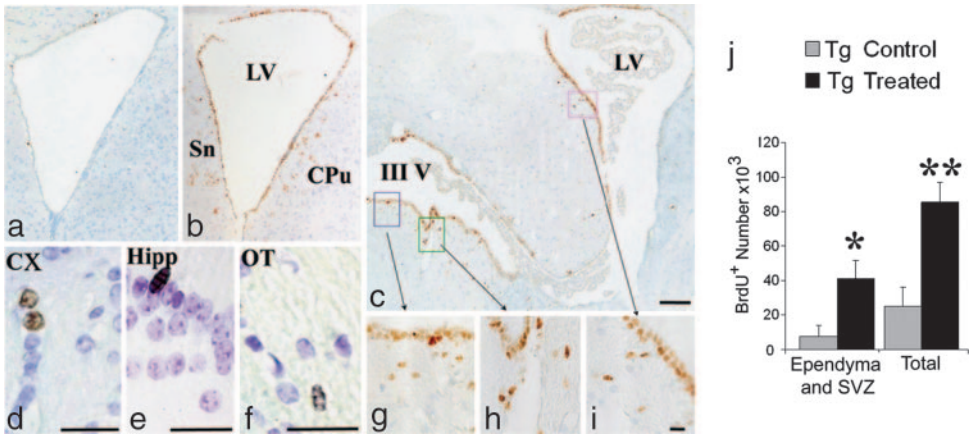

Fig. 1. Anti-EFRH immunization effects on BrdU$^+$ incorporation. Shown are BrdU$^+$ cells from Tg control (*a*) and Tg treated (*b–i*) animals. (*a–c*) BrdU$^+$ cells among the ependyma and adjacent areas of treated vs. untreated animals 0.02 from bregma (*a* and *b*) and 0.22 from bregma (*c*). (*g–i*) Enlargement of the rectangles in *c*. (*a–c* and *g–i* were counterstained with hematoxylin.) (*d–f*) BrdU$^+$ cells in the cortex (*d*), hippocampus (*e*), and optic tract (*f*) in treated animals (counterstained with thionin). Sn, septal nuclei; CPu, striatum; LV, lateral ventricle; III V, third ventricle; Cx, cortex; Hipp, hippocampus; OT, optic tract. (Scale bars: 200 μm in *c*, corresponding also to *a* and *b*; 25 μm in *d–f*; 5 μm in *i*, corresponding also to *g* and *h*.) (*j*) Total number of BrdU$^+$ cells in treated mice was approximately three times higher than in control, untreated mice. In the ependyma and SVZ it was approximately five times higher. *, $P \leq 0.05$; **, $P \leq 0.01$ (Tg Treated vs. Tg untreated).

the last BrdU injection. BrdU$^+$ cells were abundant among cells lining the ventricles (ependyma) and SVZ, particularly in the anterior horn of the lateral ventricles (Fig. 1 *a–c* and *g–i*). We considered the first row of cells facing the ventricles to be ependyma, and cells whose nuclei resided within areas of approximately three times cell diameter surrounding the ventricle to be within the SVZ. We also observed BrdU$^+$ cells in various areas of the brain, including the white and gray matter, such as cortex (Fig. 1*d*), hippocampus (Fig. 1*e*), optic tract (Fig. 1*f*), and more.

An overall elevation in the number of BrdU$^+$ cells in treated vs. untreated animals was observed, which varied according to area examined. The total number of BrdU$^+$ cells in PDAPP Tg treated mice (85,520 $\pm$ 11,518; $P \leq 0.013$) was approximately three times higher than that of PDAPP Tg control, untreated mice (25,100 $\pm$ 10,756), whereas in the cells lining the walls of ventricles it was approximately five times higher (41,040 $\pm$ 10,711 vs. 7,753 $\pm$ 6,025, respectively; $P \leq 0.05$) (Fig. 1*j*).

BrdU$^+$ Cell Phenotyping. BrdU$^+$ cell phenotypes were identified by double-labeling with either mature neuronal (NeuN) or glial [glial fibrillary acidic protein (GFAP)] markers. Double-labeled BrdU$^+$/NeuN$^+$ cells were found widely distributed in brains of both PDAPP Tg treated and untreated mice. BrdU$^+$/NeuN$^+$ cells were distributed throughout the whole brain in both gray and white matter (Fig. 2). We observed BrdU$^+$/NeuN$^+$ cells in the hippocampus (Fig. 2 *a–c*), particularly in the granular and SGZ of the DG, cortex (Fig. 2*d*), and SVZ (Fig. 2*e*). BrdU$^+$/NeuN$^+$ cells were also observed in vascular beds surrounding large blood vessels (Fig. 2*f*) and in white matter areas, such as the optic tract (Fig. 2 *g* and *h*). A significantly elevated number of double-labeled BrdU$^+$/NeuN$^+$ cells in PDAPP Tg treated mice, compared with PDAPP Tg-untreated mice, was counted in the cortex, amygdala, hippocampus, optic tract, thalamus, and ependyma and subventricular layer of the lateral ventricles (Fig. 3*a*). In other regions, such as the striatum, internal capsule, and corpus callosum, the numbers of BrdU$^+$/NeuN$^+$ cells were almost equal among the experimental groups.

The mean numerical density of the BrdU$^+$ cells in two coronal sections at the levels of -1.6 and -3.6 from the bregma was approximately two times higher in PDAPP Tg treated mice (4.2 $\pm$ 0.4 cells per square millimeter) compared with PDAPP Tg-untreated controls (2.3 $\pm$ 0.4 cells per square millimeter) ($P \leq 0.005$) (Fig. 3*b*). The mean numerical density of the double-positive BrdU$^+$/NeuN$^+$ cells in these sections was $\approx$2.5 times higher in PDAPP Tg treated mice (3.6 $\pm$ 0.4 cells per

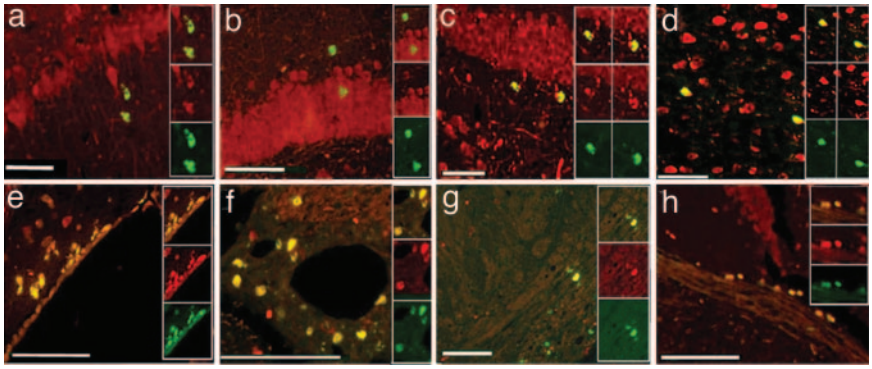

Fig. 2. Anti-EFRH immunization effects on neurogenesis. BrdU$^+$ cell phenotypes: BrdU$^+$ neuronal phenotypes were identified by double-labeling with the mature neuronal marker NeuN (green, BrdU; red, NeuN; yellow, merged). BrdU$^+$/NeuN$^+$ cells were found widely distributed in brains of both Tg treated and untreated mice in areas such as the CA1 of the hippocampus (*a*), the granular (*b*) and SGZ (*c*) of the DG, the cortex (*d*), the SVZ (*e*), the vascular beds (*f*), and the optic tract (*g* and *h*). (Scale bars: 50 μm in *a–e* and *h*, 250 μm in *f*, and 20 μm in *g*.)

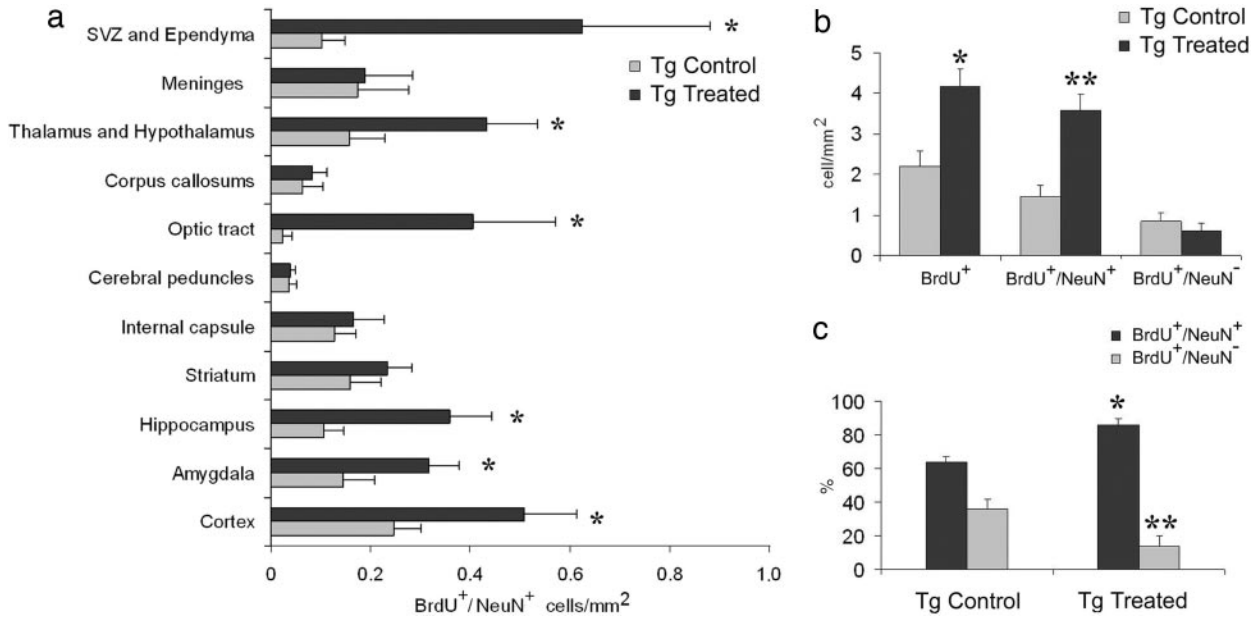

Fig. 3. Count of $BrdU^+$ and $BrdU^+$/ $NeuN^+$ double-labeled cells. (*a*) Significant elevation (*) in double-labeled $BrdU^+/NeuN^+$ numerical density was found in various areas of Tg treated vs. Tg control animals. In other regions, $BrdU^+/NeuN^+$ cells were almost equal among experimental groups. *, $P \leq 0.01$ from Tg control. (*b*) Numerical density of total number of $BrdU^+$ cells of Tg treated animals was significantly elevated compared with Tg control, untreated mice. $BrdU^+/NeuN^+$ numerical density was higher in Tg treated vs. Tg untreated mice, whereas the number of $BrdU^+$ cells with no recognized phenotype was almost equal in both groups. (*c*) EFRH immunization shifted $BrdU^+$ cells toward differentiation into neuronal phenotype. The fraction of $BrdU^+/NeuN^+$ of the total number of $BrdU^+$ cells was significantly elevated in Tg treated vs. Tg control mice. *, $P \leq 0.05$; **, $P \leq 0.01$ (compared with Tg untreated).

square millimeter) than in controls (1.45 ± 0.3 cells per square millimeter) ($P \leq 0.005$) (Fig. 3*a*), whereas that of $BrdU^+/NeuN^-$ cells was similar in PDAPP Tg treated and untreated mice (0.6 ± 0.1 and 0.84 ± 0.2 cell per square millimeter, respectively).

The fraction of $BrdU^+/NeuN^+$ cells of the total BrdU-labeled cells was significantly shifted toward the neuronal phenotype in PDAPP Tg treated mice compared with PDAPP Tg-untreated mice (90% vs. 63%, respectively) ($P \leq 0.0002$) (Fig. 3*c*). The increased numerical density of the double-labeled $BrdU^+/NeuN^+$ cells was inversely correlated with amyloid burden ($R = -0.63$; $P \leq 0.004$) and with GFAP load ($R = -0.55$; $P \leq 0.01$).

Zif268 Expression in $BrdU^+/NeuN^+$ Cells. Most of the $BrdU^+/NeuN^+$ cells were observed by confocal microscopy to be colocalized with Zif268 (Erg-1), a member of the immediate early genes (Fig. 4). Zif268 is primarily expressed after synaptic activation and therefore serves as a marker of synaptic functionality (25, 28, 29), and it has been shown to be necessary for formation of

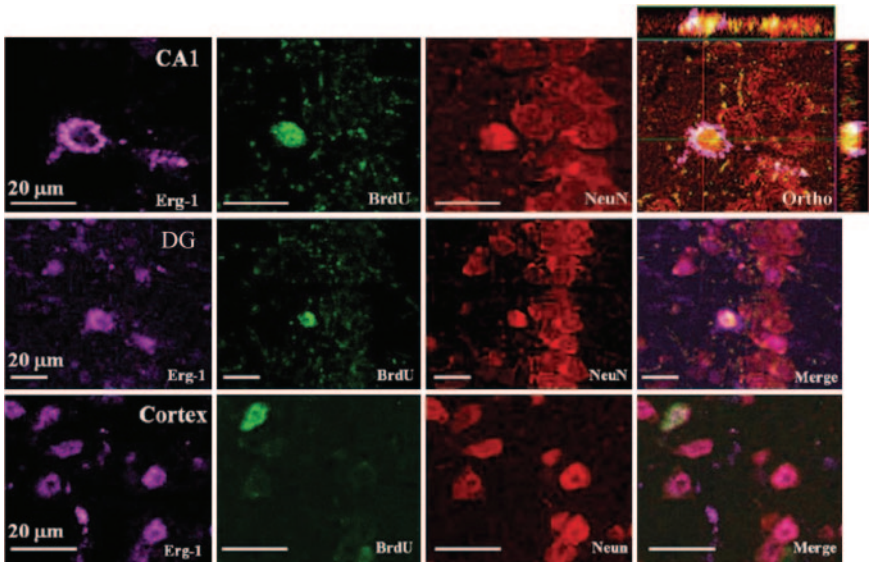

Fig. 4. Colocalization of $BrdU^+/NeuN^+$ cells with Zif268 (Erg-1). Triple-labeling with anti-BrdU, anti-NeuN, and anti-Zif268: Confocal microscopic study shows that $BrdU^+/NeuN^+$ cells were colocalized with the early expression gene Zif268. Triple-labeled cells ($BrdU^+/NeuN^+/Zif268^+$) are depicted here in hippocampal CA1, the DG, and the cortex. Ortho points at an image that was rotated in the orthogonal planes (*x*, *y*, and *z*) to verify the triple-labeling.

different forms of long-term memory (reviewed in ref. 30). The triple-labeled cells ($BrdU^+/NeuN^+/ERG1^+$) were observed in all of the aforementioned areas hosting $BrdU^+$ cells.

Discussion

AβP immunization of murine models of AD proved to be effective in AβP plaque reduction, correlated with improvement in cognitive functions (13, 14). We suggest here that the improvement in memory and learning, combined with alleviation of the neurotoxic amyloid burden and the pathology associated with it, may reflect functional neurogenesis induced by the anti-AβP immunization.

Enhanced neurogenesis has been reported in various conditions of brain insults, such as stroke (31), focal cerebral ischemia (31–33), Parkinson's disease (34), epilepsy (35), and Huntington's disease (36, 37), as well as AD (38) and in animal models of AD, such as PDGF-$APP_{Sw,Ind}$ (39), APP23 (40), and PDAPP mice (27).

Here we provide the first evidence of stimulation of endogenous neurogenesis in PDAPP Tg mice, modulated by EFRH site-directed immunization. We found a significant increase in the total number of $BrdU^+$ cells in the brains of PDAPP Tg treated mice compared with untreated animals. We did not find such an increase in $BrdU^+$ cells in the brains of PDAPP Tg mice treated with scrambled peptide.

A 3-fold elevation in the total number of $BrdU^+$ cells in treated vs. untreated animals was observed in various areas of the brain, indicating that the treatment had an effect on progenitor cell proliferation, migration, and survival. We also show a 5-fold elevation in the number of $BrdU^+$ cells lining the ventricle walls, which we considered to be ependymal cells, indicating that the treatment is directed primarily at mitogenesis/proliferation of these cells.

$BrdU^+$ cells are the direct surviving progeny of the cells that were in the S-phase during exposure to the label (41). These cells had to migrate to their destination site and complete their differentiation into mature neurons, a process that takes a few weeks (42, 43). For that reason, in the present study the mice were killed 41 days after the last BrdU labeling to let the newly born cells, which incorporated the tracer, to survive and finish migration and maturation and to integrate into the brain circuit (42–44). This time point had its pitfalls because, by confining ourselves to only one time point, we were unable to assess the balance between cell genesis and cell death. Another pitfall is the BrdU diluting factor (reviewed in ref. 41) that causes the neuroprogenitor cells, which continued to divide and to become indistinguishable and, thus, uncountable. BrdU tracer labels also some injured cells undergoing DNA repair in addition to proliferating cells, but it was reported that a standard dose of BrdU (50 mg/kg of body weight) injected into adult rodents is not sufficient for detecting DNA repair during apoptosis (45). In addition, BrdU is not cell-lineage-specific; therefore, it is important to establish $BrdU^+$ cell phenotype by staining with specific markers, such as NeuN (reviewed in ref. 41).

We demonstrate here that anti-EFRH immunization had a marked effect on progenitor cells by promoting their differentiation and maturation into neurons. In PDAPP Tg treated mice the numerical density of $BrdU^+/NeuN^+$ cells was 2.5-fold higher than in PDAPP Tg control mice. This increase was inversely correlated with amyloid burden and GFAP load alleviated by the treatment. Furthermore, in treated animals the fraction of $BrdU^+/NeuN^+$ of the total $BrdU^+$ cells was significantly shifted toward the neuronal phenotype. Because wild-type C57BL mice did not respond to immunological challenge with EFRH antigen, we were unable to correlate the anti-EFRH Abs with endogenous neurogenesis in these mice.

Despite previous assumptions that considered NSC to be confined to the SVZ and the DG, recent studies found that NSC are also widely present in nonneurogenic regions throughout the adult CNS, such as the spinal cord, cerebellum, septal and striatal parenchyma, and others (reviewed in refs. 46 and 47). Recently, Takemura (48) provided evidence for neurogenesis within the white matter (external capsule) of normal rats, termed the temporal germinal layer. However, under normal physiological conditions these cells generate glial cells. Our results also show that $BrdU^+$ cells were observed in various areas of the brain: i.e., cortex, septal nuclei, thalamus, hypothalamus, amygdala, CA1, CA3 of the hippocampus, and SGZ. In the white matter we detected cells in the corpus callosum, hippocampal commisure, fornix, alveus, fimbria, internal and external capsule, and cerebral peduncles. $BrdU^+$ cells were observed in midbrain, especially in cells lining the walls of cerebral aqueduct, periaqueductal gray, mecencephalic nuclei, the superior coliculli, superior brachium, and lateral geniculate nucleus and optic tract, as well as in the vascular bed. Most of these cells were $BrdU^+/NeuN^+$ newly born neurons. Indeed, almost all of these areas, being isolated *in vitro*, were shown to contain stem cells and have a potency for neurogenesis under appropriate physiological conditions and microenvironmental factors (49, 50).

It was previously proposed that adult-generated neurons might be involved in normal functions of areas to which they were added. New cells in the DG may play a role in hippocampal modulation of memory (51); new cells in the hypothalamus may be involved in energy balance (52). Similarly, newly generated neurons in the olfactory bulb were integrated into the neural circuitry involved in processing sensory input (53). Here we provide evidence that the newly born neurons mature and start to participate in activity-dependent protein expression because most of the $BrdU^+/NeuN^+$ cells expressed Zif268, a marker of functionality (25, 28, 29). We therefore show that anti-EFRH immunization of PDAPP Tg mice generated newly born neurons that can respond to synaptic input and, thus, may have been properly incorporated into the brain.

The mechanism of anti-EFRH modulatory effect on neurogenesis is still under investigation and might be explained according to a few reported data regarding the role of AβP as a neurotrophic and/or neurotoxic agent. One possible explanation stems from recently reported studies depicting the benefits of AβP. Lopez-Toledano and Shelanski (54) showed that AβP increases neurogenesis in hippocampal stem cell culture in a dose-dependent manner, suggesting that formation of new neurons is more likely to be induced by "soluble" forms of AβP. Therefore, the beneficial effect of anti-EFRH treatment might stem from the neurogenic effect of the soluble forms of AβP, which remain after disaggregation and removal of aggregated dense plaques by these Abs, as well as from clearance of excess AβP (16, 20–24, 55, 56).

The second possible explanation arises from recent studies (57, 58), where human AβP, injected into the lateral ventricle, inhibited long-term potentiation in rat hippocampus *in vivo*. This effect was completely reversed by a mAb to AβP, suggesting that Abs to AβP can exert a beneficial effect by directly neutralizing potentially synaptotoxic soluble AβP species in the brain. The high correlation between increased neurogenesis in PDAPP Tg treated mice and reduction in amyloid burden (SI Fig. 5*I*) advocate this hypothesis, which nevertheless still needs to be proved.

A third possible explanation of the beneficial effect on neurogenesis stimulation in anti-EFRH-treated PDAPP Tg mice may correspond to alleviation of neuroinflammation (SI Fig. 5 *II* and *III*), exhibited as reduced astrocytic and microglial activation. Brain inflammation causes inhibition of neurogenesis (59, 60), and precursor cells tend to become astrocytes rather than neurons under conditions of chronic inflammation (61). Therefore, the anti-EFRH immunization, which significantly reduced brain GFAP and F4/80, a marker of activated microglia, may promote generation of neuronal precursor cells and, fur-

thermore, lead them toward maturation. All of these arguments favor neurogenesis, and there seems to be a combination of effects, resulting from neutralization and clearance of such neurotoxic AβP species, until the "neurotrophic" concentration of AβP is reached.

Recently, similar results demonstrating the neurogenic effect of drugs used to treat cognitive impairment in a Tg mice model of AD, AChE inhibitors and an NMDA antagonist (tacrine, galantamine, and memantine), were shown *in vitro* and *in vivo* (62). All of these treatments potentiated neurogenesis in the two principal neuroproliferative regions of the rodent brain: the SGZ and the forebrain SVZ.

Increased neurogenesis in DG from patients with AD was reported (38) and was proposed to represent a response to injury that is directed at brain repair, but progressive cell loss was still observed. If pathological features of AD trigger increased neurogenesis, then one mechanism through which AD treatments might produce symptomatic improvement might be by augmenting this effect. Indeed, the AD patients treated with AN1792 in the first Elan/Wyeth clinical trials showed that Ab responders had a more pronounced reduction in brain volume than nonresponders, and this reduction in brain volume is associated with better cognitive performance (63). These volume changes may be due to amyloid removal. In our experiments we measured volume of brain and hippocampi and found reduction in brain volume, but not in the hippocampus, which brought about an elevation in the percentage of volume occupied by the hippocampus in treated vs. untreated animals (data not shown).

In conclusion, anti-EFRH Abs stimulate endogenous neurogenesis and can thus contribute to recovery from AD and other neurodegenerative diseases related to AβP overproduction and neurotoxicity, bearing hope for future treatment. Despite the fact that the mechanism of the anti-EFRH vaccination effect on neurogenesis is still under investigation, this report suggests that AβP immunotherapy can stimulate formation of new functional neurons in brains of Tg treated mice, which may be associated with improvement in cognition.

Materials and Methods

Animals. Four-month-old male and female APP^{V717F} heterozygous Tg mice (PDAPP) were provided by Elan Pharmaceuticals (South San Francisco, CA). PDAPP mice were produced on a Swiss–Webster$\times B_6D_2F_1$ (C57BL/6$\times$DBA/2) outbreed background (26). In parallel, wild-type C57BL mice were used as control. Mice were maintained under a 12-h light/12-h dark cycle, with rodent chow (Koffolk, Tel-Aviv, Israel) and water provided ad libitum. The animals were housed 5–10 per cage in a room maintained at 22 $\pm$ 0.5°C under laminar flow. All procedures performed were reviewed and approved by the Animal Care and Use Committee of Tel-Aviv University before initiation of the study.

Immunization Procedure. EFRH and scrambled EFRH peptides were used as the antigens for immunization. Because of poor immunogenicity, we prepared multiple antigenic peptide with 16 copies of the antigens. For immunization, the antigens were emulsified with 2 volumes of complete (for primary immunization) or incomplete (for following boosts) Freund's adjuvant (Difco Laboratories, Detroit, MI). Four-month-old PDAPP Tg mice ($n = 12$) were immunized by i.p. injection of 100 μg of antigens five times, once every 2 weeks. Two additional boosts were injected at 12 and 13 months of age.

BrdU Labeling. At the age of 14 months, all PDAPP Tg mice were injected i.p. once per week for 4 weeks with 0.1 ml of BrdU per 100 g of body weight (Zymed/Invitrogen, Carlsbad, CA). Mice were killed 41 days after the last BrdU injection.

Abs. All Abs were diluted in TBS (pH 7) containing 0.1% Triton X-100 and 0.05% Tween 20. Primary Abs were supplemented with 3% donkey serum. The primary Abs used were as follows: rabbit anti-GFAP (1:1,000; DAKO/Cytomation, Glostrup, Denmark), mouse anti-neuron-specific nuclear protein (NeuN, 1:200; Zymed), rat anti-F4/80 (1:100; Serotec, Oxford, U.K.), sheep anti-BrdU (1:200; Biodesign International, Saco, ME), and rabbit anti-Zif268 (1:200; Santa Cruz Biotechnology, Santa Cruz, CA).

The following secondary Abs used were purchased from Zymed: broad-range polymer HRP (Picture Plus kit) or biotinylated goat anti-rat HRP followed by avidin-HRP, which were developed by 3,3-diaminobenzedine tetrahydrochloride (Zymed). The following secondary fluorescent Abs were used: goat anti-mouse Cy3 and goat anti-rabbit Cy5 (1:500; Jackson ImmunoResearch Laboratories, West Grove, PA), goat anti-mouse Alexa Fluor 546, and donkey anti-sheep Alexa Fluor 488 (1:200; Molecular Probes, Carlsbad, CA).

Neuropathological Evaluation. At 16 months of age all animals were deeply anesthetized with ether and intracardially perfused with 4% paraformaldehyde (Sigma, Rehovot, Israel) in 0.01 M phosphate buffer (pH 7.4) containing 5 units/ml heparin (Sigma). The brains were excised and further postfixed with the same fixative overnight at 4°C. Brains were dehydrated and embedded in paraffin. Serial coronal sections (5 μm) were taken in an anterior-to-posterior direction 300 μm apart from each other. Sections were then prepared for histological and immunohistochemical evaluation.

Light Microscopy. Bright-field and fluorescent signals were detected by using a Leica (Wetzler, Germany) DMLB microscope and a LS510 Zeiss (Jena, Germany) confocal microscope.

Counting of $BrdU^+$ Cells. Sections were quenched by 3% H_2O_2 in methanol for 5 min at room temperature. BrdU-incorporated cells ($BrdU^+$) were detected by a biotinylated mAb against BrdU, followed by streptavidin-HRP (BrdU staining kit; Zymed) according to the manufacturer's instructions. Sections then were exposed to 3,3-diaminobenzedine tetrahydrochloride and counterstained with hematoxylin. As a negative control we omitted the first Ab, and as positive controls we used sections of gut and spleen of mice that had been daily injected with BrdU for a week and killed 30 min after the last injection.

Quantification of $BrdU^+$ Cells Along the Hemisphere. Microscopic evaluation was performed at a magnification of $\times$400. The total number of $BrdU^+$ cells in the left hemisphere was estimated by using unbiased stereological counting methods (42, 64). $BrdU^+$ cells in each hemisphere were counted in three control and three treated animals by a blind-to-treatment investigator in serial (anterior to posterior) coronal brain sections, taken every 300 μm from area 0.5 to area -3.6 to -3.8 from the bregma. The total number of $BrdU^+$ cells (N) was estimated in each hemisphere by multiplying the sum of cells in each of the series of 5-μm sections ($\Sigma N_{\text{counted cells}}$) by the sampling fraction (k). Because every 60th section was used for counting, the sampling fraction was $k = 60$; thus, the total number was calculated by multiplying the sum of the cells in each of the series by 60.

Evaluation of $BrdU^+$ Phenotype. For this purpose we examined the colocalization of BrdU incorporation with NeuN, a marker of mature, differentiated neurons, and with the early functional gene Zif268 in the $BrdU^+$ cells, as a marker for synaptic functionality in neurons (25, 28, 65).

For immunofluorescent double (sheep anti-BrdU and mouse anti-NeuN) and triple (sheep anti-BrdU, mouse anti-NeuN, and rabbit anti-Zif268) labeling, we used paraffin sections (5 μm),

which were microwaved in 0.01 M TBS (pH 9.0) containing 0.005 M EGTA and boiled for 15 min. After cooling, sections were blocked with Ultra-V block (Lab Vision, Fremont, CA) and incubated with the mixture of first Abs overnight at 4°C. After rinses in TBS, the sections were incubated consecutively for 1 h at room temperature with anti-sheep Ab conjugated to Alexa Fluor 488, anti-mouse Ab conjugated to Cy3 or Alexa Fluor 546, and anti-rabbit Ab conjugated to Cy5. Sections were washed with TBS (pH 8.0) and mounted in anti-fade mounting media containing 0.25% 1,4-diazabicyclo-(2,2,2)-octane (Sigma) and 5% propyl gallate (Sigma) in glycerol.

Quantification of Double and Triple Immunolabeling. $BrdU^+$ cells were counted by a blind-to-treatment investigator in two coronal sections at the levels of −1.6 and −3.6 from the bregma, respectively, using a fluorescent microscope at a magnification of ×630. Images were obtained via a CCD color video camera (ProgRes C14; Jenoptic, Jena, Germany). $BrdU^+$ cell double-labeling with NeuN was verified by obtaining two images, using a 580-nm filter for Cy3 and a 480-nm filter for Alexa Fluor 488, from each studied frame. The images were composed by using PhotoStudio 2000 (ArcSoft, Fremont, CA) software, and double-labeled cells were counted. The numerical densities of all $BrdU^+$, $BrdU^+$/$NeuN^+$, and $BrdU^+$/$NeuN^-$ cells were calculated as the number of cells per square millimeter of brain section. Using 5-μm sections, the chance of false positive detection of two overlapping cells, one expressing BrdU and the other expressing NeuN, was very slim. Expression of the immediate early gene Zif268 colocalized with BrdU and NeuN was studied in all $BrdU^+$ cells in each section by using the confocal microscope.

Statistical Analyses. Data are presented in the text as mean ± SEM. Statistical differences between groups were determined by a two-tailed t test, with planned comparisons between groups (Tg control vs. Tg treated). For analysis of three and more variables we used one-way ANOVA followed by post hoc comparison testing. Correlations between variables were determined by linear regression analysis. For all analyses, $P \leq 0.05$ was considered significant. Statistical analyses were performed by using SPSS software (SPSS, Chicago, IL).

We thank Nurit Haimovitz for excellent help in preparing histological specimens and Faybia Margolin for help with manuscript preparation.

1. Kempermann G, Jessberger S, Steiner B, Kronenberg G (2004) *Trends Neurosci* 27:447–452.
2. Alvarez-Buylla A (1997) *Semin Cell Dev Biol* 8:207–213.
3. Kornack DR, Rakic P (2001) *Proc Natl Acad Sci USA* 98:4752–4757.
4. Lois C, Alvarez-Buylla A (1994) *Science* 264:1145–1148.
5. Luskin MB (1993) *Neuron* 11:173–189.
6. Abrous DN, Koehl M, Le Moal M (2005) *Physiol Rev* 85:523–569.
7. Cameron HA, Woolley CS, McEwen BS, Gould E (1993) *Neuroscience* 56:337–344.
8. Madsen TM, Kristjansen PE, Bolwig TG, Wortwein G (2003) *Neuroscience* 119:635–642.
9. Monje ML, Palmer T (2003) *Curr Opin Neurol* 16:129–134.
10. Selkoe DJ (2001) *Physiol Rev* 81:741–766.
11. Hardy J, Selkoe DJ (2002) *Science* 297:353–356.
12. Selkoe DJ, Schenk D (2003) *Annu Rev Pharmacol Toxicol* 43:545–584.
13. Morgan D, Diamond DM, Gottschall PE, Ugen KE, Dickey C, Hardy J, Duff K, Jantzen P, DiCarlo G, Wilcock D, *et al.* (2000) *Nature* 408:982–985.
14. Janus C, Pearson J, McLaurin J, Mathews PM, Jiang Y, Schmidt SD, Chishti MA, Horne P, Heslin D, French J, *et al.* (2000) *Nature* 408:979–982.
15. Hock C, Konietzko U, Streffer JR, Tracy J, Signorell A, Muller-Tillmanns B, Lemke U, Henke K, Moritz E, Garcia E, *et al.* (2003) *Neuron* 38:547–554.
16. Solomon B, Koppel R, Frankel D, Hanan-Aharon E (1997) *Proc Natl Acad Sci USA* 94:4109–4112.
17. Bard F, Cannon C, Barbour R, Burke RL, Games D, Grajeda H, Guido T, Hu K, Huang J, Johnson-Wood K, *et al.* (2000) *Nat Med* 6:916–919.
18. DeMattos RB, Bales KR, Cummins DJ, Dodart JC, Paul SM, Holtzman DM (2001) *Proc Natl Acad Sci USA* 98:8850–8855.
19. Morgan D (2005) *Neurodegener Dis* 2:261–266.
20. Frenkel D, Balass M, Solomon B (1998) *J Neuroimmunol* 88:85–90.
21. Frenkel D, Balass M, Katchalski-Katzir E, Solomon B (1999) *J Neuroimmunol* 95:136–142.
22. Solomon B, Koppel R, Hanan E, Katzav T (1996) *Proc Natl Acad Sci USA* 93:452–455.
23. Frenkel D, Dewachter I, Van Leuven F, Solomon B (2003) *Vaccine* 21:1060–1065.
24. Lavie V, Becker M, Cohen-Kupiec R, Yacoby I, Koppel R, Wedenig M, Hutter-Paier B, Solomon B (2004) *J Mol Neurosci* 24:105–113.
25. Bozon B, Davis S, Laroche S (2002) *Hippocampus* 12:570–577.
26. Games D, Adams D, Alessandrini R, Barbour R, Borthelette P, Blackwell C, Carr T, Clemens J, Donaldson T, Gillespie F, *et al.* (1995) *Nature* 373:523–527.
27. Donovan MH, Yazdani U, Norris RD, Games D, German DC, Eisch AJ (2006) *J Comp Neurol* 495:70–83.
28. Jessberger S, Kempermann G (2003) *Eur J Neurosci* 18:2707–2712.
29. Steiner H, Kitai ST (2000) *J Neurosci* 20:5449–5460.
30. Guzowski JF (2002) *Hippocampus* 12:86–104.
31. Arvidsson A, Collin T, Kirik D, Kokaia Z, Lindvall O (2002) *Nat Med* 8:963–970.
32. Jin K, Minami M, Lan JQ, Mao XO, Batteur S, Simon RP, Greenberg DA (2001) *Proc Natl Acad Sci USA* 98:4710–4715.
33. Felling RJ, Levison SW (2003) *J Neurosci Res* 73:277–283.
34. Fallon J, Reid S, Kinyamu R, Opole I, Opole R, Baratta J, Korc M, Endo TL, Duong A, Nguyen G, *et al.* (2000) *Proc Natl Acad Sci USA* 97:14686–14691.
35. Parent JM, Yu TW, Leibowitz RT, Geschwind DH, Sloviter RS, Lowenstein DH (1997) *J Neurosci* 17:3727–3738.
36. Curtis MA, Penney EB, Pearson J, Dragunow M, Connor B, Faull RL (2005) *Neuroscience* 132:777–788.
37. Curtis MA, Penney EB, Pearson AG, van Roon-Mom WM, Butterworth NJ, Dragunow M, Connor B, Faull RL (2003) *Proc Natl Acad Sci USA* 100:9023–9027.
38. Jin K, Peel AL, Mao XO, Xie L, Cottrell BA, Henshall DC, Greenberg DA (2004) *Proc Natl Acad Sci USA* 101:343–347.
39. Jin K, Galvan V, Xie L, Mao XO, Gorostiza OF, Bredesen DE, Greenberg DA (2004) *Proc Natl Acad Sci USA* 101:13363–13367.
40. Bondolfi L, Calhoun M, Ermini F, Kuhn HG, Wiederhold KH, Walker L, Staufenbiel M, Jucker M (2002) *J Neurosci* 22:515–522.
41. Prickaerts J, Koopmans G, Blokland A, Scheepens A (2004) *Neurobiol Learn Mem* 81:1–11.
42. Kempermann G, Gast D, Kronenberg G, Yamaguchi M, Gage FH (2003) *Development (Cambridge, UK)* 130:391–399.
43. van Praag H, Schinder AF, Christie BR, Toni N, Palmer TD, Gage FH (2002) *Nature* 415:1030–1034.
44. Markakis EA, Gage FH (1999) *J Comp Neurol* 406:449–460.
45. Cooper-Kuhn CM, Kuhn HG (2002) *Brain Res Dev Brain Res* 134:13–21.
46. Picard-Riera N, Nait-Oumesmar B, Baron-Van Evercooren A (2004) *J Neurosci Res* 76:223–231.
47. Emsley JG, Mitchell BD, Kempermann G, Macklis JD (2005) *Prog Neurobiol* 75:321–341.
48. Takemura NU (2005) *Neuroscience* 134:121–132.
49. Magavi SS, Macklis JD (2002) *Brain Res Dev Brain Res* 134:57–76.
50. Emsley JG, Mitchell BD, Magavi SS, Arlotta P, Macklis JD (2004) *NeuroRx* 1:452–471.
51. Shors TJ (2004) *Trends Neurosci* 27:250–256.
52. Kokoeva MV, Yin H, Flier JS (2005) *Science* 310:679–683.
53. Carleton A, Petreanu LT, Lansford R, Alvarez-Buylla A, Lledo PM (2003) *Nat Neurosci* 6:507–518.
54. Lopez-Toledano MA, Shelanski ML (2004) *J Neurosci* 24:5439–5444.
55. Frenkel D, Solomon B, Benhar I (2000) *J Neuroimmunol* 106:23–31.
56. Frenkel D, Katz O, Solomon B (2000) *Proc Natl Acad Sci USA* 97:11455–11459.
57. Klyubin I, Walsh DM, Lemere CA, Cullen WK, Shankar GM, Betts V, Spooner ET, Jiang L, Anwyl R, Selkoe DJ, Rowan MJ (2005) *Nat Med* 11:556–561.
58. Rowan MJ, Klyubin I, Wang Q, Anwyl R (2005) *Biochem Soc Trans* 33:563–567.
59. Monje ML, Toda H, Palmer TD (2003) *Science* 302:1760–1765.
60. Ekdahl CT, Claasen JH, Bonde S, Kokaia Z, Lindvall O (2003) *Proc Natl Acad Sci USA* 100:13632–13637.
61. Kwak YD, Brannen CL, Qu T, Kim HM, Dong X, Soba P, Majumdar A, Kaplan A, Beyreuther K, Sugaya K (2006) *Stem Cells Dev* 15:381–389.
62. Jin K, Xie L, Mao XO, Greenberg DA (2006) *Brain Res* 1085:183–188.
63. Fox NC, Black RS, Gilman S, Rossor MN, Griffith SG, Jenkins L, Koller M (2005) *Neurology* 64:1563–1572.
64. West MJ (1999) *Trends Neurosci* 22:51–61.
65. Williams JM, Beckmann AM, Mason-Parker SE, Abraham WC, Wilce PA, Tate WP (2000) *Brain Res Mol Brain Res* 77:258–266.